

**Direct analysis of aldehydes and carboxylic acids in the
gas phase by negative ionization SIFT-MS:
quantification and modeling of ion-molecule reactions**

Mylène Ghislain, Nathalie Costarramone, Jean-Marc Sotiropoulos, Thierry Pigot, Robin van den Berg, Sylvie Lacombe-Lhoste, Mickael Le Béché

► **To cite this version:**

Mylène Ghislain, Nathalie Costarramone, Jean-Marc Sotiropoulos, Thierry Pigot, Robin van den Berg, et al.. Direct analysis of aldehydes and carboxylic acids in the gas phase by negative ionization SIFT-MS: quantification and modeling of ion-molecule reactions. *Rapid Communications in Mass Spectrometry*, Wiley, 2019, 33 (21), pp.1623-1634. 10.1002/rcm.8504 . hal-02187657

HAL Id: hal-02187657

<https://hal.archives-ouvertes.fr/hal-02187657>

Submitted on 30 Nov 2020

HAL is a multi-disciplinary open access archive for the deposit and dissemination of scientific research documents, whether they are published or not. The documents may come from teaching and research institutions in France or abroad, or from public or private research centers.

L'archive ouverte pluridisciplinaire **HAL**, est destinée au dépôt et à la diffusion de documents scientifiques de niveau recherche, publiés ou non, émanant des établissements d'enseignement et de recherche français ou étrangers, des laboratoires publics ou privés.

Direct analysis of aldehydes and carboxylic acids in the gas phase by negative ionization SIFT-MS: quantification and modeling of ion-molecule reactions

Mylène Ghislain,^{a,b} Nathalie Costarramone,^c Jean-Marc Sotiropoulos,^a Thierry Pigot,^a
Robin Van Den Berg,^b Sylvie Lacombe,^a Mickael Le Behec^{a*}

^a CNRS/ Univ. Pau & Pays Adour/ E2S UPPA, IPREM, Institut des sciences analytiques et de Physicochimie pour l'environnement et les Matériaux, UMR5254, Hélioparc, 2 avenue Président Angot, 64053, PAU cedex 9, France

^b Intersciences Nederlands, Tijkstraat 16, 4823 AA Breda

^c UT2A, 2 avenue Président Angot, 64053, PAU cedex 9, France

* Correspondence to : Mickael Le Behec, CNRS/ Univ. Pau & Pays Adour/ E2S UPPA, IPREM, Institut des sciences analytiques et de Physicochimie pour l'environnement et les Matériaux, UMR5254, Hélioparc, 2 avenue Président Angot, 64053, PAU cedex 9, France

e-mail : mickael.lebehec@univ-pau.fr

Abstract

RATIONALE

The concentrations of aldehydes and volatile fatty acids have to be controlled because of their potential harmfulness in indoor air or relationship with the organoleptic properties of agri-food products. Although several specific analytical methods are currently used, their simultaneous analysis in a complex matrix remains a challenge. The combination of positive and negative ionization SIFT-MS allows the accurate, sensitive and high frequency analysis of complex gas mixtures of these compounds.

METHODS

The ion-molecule reactions of negative precursor ions (OH^- , O^\bullet , O_2^\bullet , NO_2^- and NO_3^-) with five aldehydes and four carboxylic acids was investigated in order to provide product ions and rate constants for the quantification of these compounds by negative SIFT-MS. The results were compared to conventional analysis methods and/or to already implemented SIFT-MS positive ionization methods. The modeling of hydroxide ion (OH^-)/molecule reaction paths by ab-initio calculation allowed a better understanding of these gas phase reactions.

RESULTS

Deprotonation systematically occurs by reaction between negative ions and aldehydes or acids, leading to the formation of $[\text{M}-\text{H}]^-$ primary ions. Ab-initio calculations demonstrated the α C-H deprotonation of aldehydes and the acidic proton abstraction for fatty acids. For aldehydes, the presence of water in the flow tube leads to the formation of hydrated ions, $[\text{M}-\text{H}]^- \cdot \text{H}_2\text{O}$. With NO_2^- precursor, a second reaction channel results in ion-molecule association with the formation of $\text{M} \cdot \text{NO}_2^-$ ions.

CONCLUSIONS

Except formaldehyde, all the studied compounds can be quantified by SIFT-MS negative ionization with significant rate constants. In addition to positive ionization SIFT-MS with H_3O^+ , O_2^+ and NO^+ , negative ionization with O^\bullet , O_2^\bullet , OH^- , NO_2^- and NO_3^- extend the

range of analysis of aldehydes and carboxylic acids in air without preparation or separation step. This methodology was illustrated by the simultaneous quantification in single scan experiments of 7 aldehydes and 6 carboxylic acids released by building materials.

Keywords

Selected Ion Flow Tube – Mass Spectrometry; SIFT-MS; negative ionization; aldehydes; volatile fatty acids; modeling

Introduction

Indoor air quality is strongly affected by the presence of volatile pollutants such as formaldehyde, acetaldehyde, propanal, pentanal, hexanal, octanal, and nonanal. Among the Volatile Organic Compounds (VOC) found in indoor air, these aldehydes are the most frequent and at high concentrations ¹. The most abundant formaldehyde, together with acetaldehyde and hexanal are detected in 100 % of French dwellings ². Due to their possible impact on human health the monitoring of these compounds in indoor air is of major interest.^{3,4} The main indoor sources of aldehydes are building materials, paints and furniture, as shown by the numerous papers dealing with emissions of aldehydes in air by materials ^{1,5-7}. Outdoors, aldehydes are released into the atmosphere by vehicle exhaust and incomplete combustion of hydrocarbons ⁸.

Besides aldehydes, carboxylic acids (propanoic acid, hexanoic acid) can be produced in indoor air by reactions involving ozone and are also highly studied in outdoor air ⁸⁻¹⁰. These compounds are released into the environment from natural biodegradation and anthropogenic sources including land spreading of manure slurry involving odour nuisances ¹¹⁻¹³.

Aldehydes and carboxylic acids, individually or simultaneously, are also widely found in the volatile fraction of agri-food products. Actually, the volatile compounds emitted by agri-food products contribute to their organoleptic qualities and constitute a chemical fingerprint specifically identifying a product, qualifying a process or an evolution of the product ¹⁴⁻¹⁷. For example, butyric acid is an important indicator of cheese quality and its formation during ripening can lead to swelling, undesired slits or even a rancid taste ¹⁸. For this kind of application, aldehydes and carboxylic acids are no longer studied as pollutants but rather as potential markers at very low concentrations requiring sensitive analysis techniques. In disease diagnosis, these compounds are also monitored at trace levels as potential health markers: for instance, acetaldehyde is a common breath metabolite.^{19,20}

Therefore, due to health, economic and societal issues, the development of a common universal and fast method of analysis for the quantification of aldehydes and carboxylic acids in air in various field is of great interest.

In the literature, many methods describe the measurement of these compounds in air, as detailed below. Standard methods to measure aldehydes are based on their collection by active or passive sampling on cartridges, badges or tubes impregnated with DNPH (2,4-dinitrophenylhydrazine) followed by a solvent extraction prior to High Performance Liquid Chromatography (HPLC) analysis ²¹⁻²³. These methods are specific to the analysis of aldehydes and ketones. Others active sampling techniques followed by ion chromatography are particularly suitable for the analysis of carboxylic acids such as formic and acetic acids ²⁴.

More exhaustive methods based on Gas Chromatography – Mass spectrometry (GC-MS) techniques^{25,26}, such as Solid Phase Micro extraction (SPME) on-fiber derivatization with O-(2,3,4,5,6-pentafluorobenzyl) hydroxylamine allow the simultaneous measurement of aldehydes and others VOCs including carboxylic acids²⁷. In the food industry, gas chromatography coupled to olfactometry (GC-O) is a well-known technique for the analysis of odor active compounds such as aldehydes and volatile fatty acids²⁸. But these different methods are time consuming, complex, or highly specific. They include a separation step and are not always adapted to high frequency analysis and to the general analytical requirements previously described.

Selected Ion Flow Tube–Mass Spectrometry (SIFT-MS) and Proton Transfer Reaction–Mass Spectrometry (PTR-MS) are well-established direct injection mass spectrometry methods for direct and rapid analysis of (VOCs) with typical detection limits ranging from parts-per-billion (ppbv) to parts-per-trillion (pptv) by volume in the gas phase depending on the instruments.^{29,30} They are currently widely applied in the biological^{19,31,32}, medical^{33–35}, food^{14,36–39} and environmental fields^{11,13,40,41} because of their high frequency analysis rate and ease of use. Thus, PTR-MS and SIFT-MS techniques appear to be relevant methods instead of time-consuming chromatographic and/or derivatization ones for the analysis of aldehydes and carboxylic acids in air.

SIFT-MS technology uses softer chemical ionization than PTR-MS due to the lower pressure of the carrier gas in the flow tube (about 0.4 vs 1.5 torrs²⁹ respectively). In the SIFT-MS technique no electric field is employed (in contrast to PTR-MS) and it is thus possible to carry out ion-molecule reactions under thermal conditions where the kinetic behavior is well known.^{42,43} The other fundamental difference between these two techniques is that SIFT-MS instrument can generate eight reagent ions (H_3O^+ , O_2^+ , NO^+ , O^\bullet , O_2^\bullet , OH^- , NO_2^- and NO_3^-) as standard in the microwave-discharge plasma. PTR-MS is based on reactions with H_3O^+ ion generated with a hollow-cathode discharge although a new Switchable Reagent Ion source (SRI-PTR-MS) now allows some PTR-MS instruments to use also O_2^+ and NO^+ as reagent ions^{29,44}. PTR-MS is known as a high sensitivity and time resolution method. Until recently, in SIFT-MS instruments, only positive ionization using H_3O^+ , O_2^+ and NO^+ precursor ions was available. However, the recent development of a negative ionization source, using O^\bullet , OH^- , O_2^\bullet , NO_2^- and NO_3^- precursor ions, extended the range of analysable compounds and added a significant advantage in the discrimination of isobaric compounds⁴⁵. While methods using positive reagent ions may be used for the measurement of aldehydes and carboxylic acids^{13,46}, to the best of our knowledge, only one paper dealt with negative ionization SIFT-MS⁴⁵ and negative ion-molecule reactions in the flow tube are poorly investigated. An alternative method, multi-reagent chemical ionisation mass spectrometry (CIMS) with both positive and negative reagent ions was recently investigated as a low detection limit and high time resolution analysis of gas phase hydrogen peroxide and methyl peroxide⁴⁷. However this Atmospheric Pressure Chemical Ionization (APCI) technique suffers from low ionization efficiency and interferences arising from the formation of adducts^{29,47}. Thus, the present work aims to study the potential contribution of SIFT-MS negative ionization for the simultaneous, sensitive and high frequency detection and quantification of aldehydes and carboxylic acids in air. In addition to SIFT-MS experiments, a theoretical/computational approach was used for a better understanding of OH^- ion-molecule reactions in the flow tube and for the possible prediction of the reactivity of these two families of compounds.

Experimental section

1 – Instrument

A Voice 200 Ultra SIFT-MS instrument (SYFT Technologies, Christchurch, New Zealand), which can use both positive and negative soft ionizing reagent ions (H_3O^+ , NO^+ , O_2^+ , O^+ , OH^- , $\text{O}_2^{\bullet-}$, NO_2^- and NO_3^-) in a single scan was used in this study. Reagent ions (or precursors) are generated by microwave discharge through dry air and water at low pressure. Each precursor ion is sequentially selected by a first quadrupole mass filter and injected into the flow tube. The sample is introduced with the carrier gas (Nitrogen) in the flow tube through a heated inlet line (100°C) with a flow rate of 20 mL min^{-1} . In full scan mode (qualitative), all the ions generated in the flow tube are counted producing thus a mass spectrum over a given range of mass to charge ratios ($m/z \leq 450$). In single ion monitoring (SIM) mode (quantitative), only selected product ions and unreacted precursors are monitored and sampled into a second quadrupole mass filter.

The software (LabSyft 1.6.2, SYFT Technologies, Christchurch, New Zealand) instantaneously calculates each analyte's absolute concentration according to the following calculation, assuming that the reagent ions R^+ or R^- are in large excess relative to the product ion P^+ or P^- (Eq. 1):

$$[A] = \gamma \frac{[P^+]}{[R^+]^k} \text{ or } [A] = \gamma \frac{[P^-]}{[R^-]^k} \quad (\text{Eq. 1})$$

with

[A]: analyte concentration in the flow tube

γ : instrument calibration factor

[P^+] or [P^-]: product ion concentration in the flow tube

[R^+] or [R^-]: reagent ion concentration in the flow tube

k : reaction rate constant

The knowledge of the reactions between analytes and reagent ions in the flow tube and of their rate constants k is thus necessary for the quantification. In this work, the contribution of negative ionization for the analysis of aldehydes and carboxylic acids was investigated. The already known positive ionization mode (reaction rate constants defined in the software database) was used to monitor the analyte concentrations generated.

2 – Gaseous atmospheres generation

Acetaldehyde ($\geq 99\%$), butanal ($\geq 96\%$), hexanal (98%), benzaldehyde ($\geq 99\%$), formic acid ($\geq 95\%$), acetic acid ($\geq 99\%$), butyric acid ($\geq 99\%$) and caproic acid ($\geq 99\%$) were supplied by Sigma-Aldrich (St. Louis, MO, USA). A formaldehyde solution (37% wt. in water, containing 10-15% methanol as stabilizer, provided by Sigma-Aldrich) was used to generate formaldehyde gas.

To investigate the product ions formed by negative ion-molecule reactions, it is necessary to introduce in the flow tube each individual pure compound. Gaseous atmospheres of aldehydes (except formaldehyde) and carboxylic acids were generated by spiking aqueous

solutions, prepared from pure liquid compounds, into 1L Tedlar bag (Zefon International, Inc, Ocala, Florida, USA) or into 1L glass bottles (Duran group, Germany) filled with clean air Zero (supplied by a F-DGS (91055 Evry, France) air Zero generator) via a septum. All the analytes are thus introduced under identical conditions in the same gas matrix at about 20% RH (relative humidity). Screw cap with three GL14 ports (Duran group, Germany) were used to connect the bottles directly to the SIFT-MS instrument via the sample inlet. A Tedlar bag (Zefon International, Inc, Ocala, Florida, USA) at the bottle inlet was used to compensate the depression in the bottle during SIFT-MS sampling at a flow rate of 20 mL min⁻¹. Both permeation tube and aqueous solution were used to generate several concentrations of formaldehyde. Formaldehyde gas standard was generated using a permeation tube of paraformaldehyde (Dynacal®, VICI Metronics, 26295 Twelve Trees Poulsbo, WA 98370, USA) placed into a PUL 200 permeameter (Calibrage, Saint Chamas, France) flushed with nitrogen flow. Sampling was done by connecting directly the outlet of the permeameter to the SIFT-MS instrument sample inlet. Temperature and nitrogen flow were adjusted to obtain different concentration levels. DNPH cartridges (Sigma-Aldrich, Saint Louis, MO, USA) used to control the permeameter output concentrations confirmed the consistency of the positive mode calibration of formaldehyde (Supplementary Information, Figure S1).

3 – Identification of the product ions in negative ionization

In order to determine the product ions formed in the flow tube, full scan mass spectra were recorded with each individual compound for each precursor ion ($\text{O}^{\bullet-}$, OH^- , $\text{O}_2^{\bullet-}$, NO_2^- and NO_3^-) in a m/z range from 12 to 250 with an integration time of 120 s. Under these conditions, different ions can be observed arising from the analyte but also from water, carbon dioxide and dioxygen introduced at the same time in the flow tube. Accordingly, water, carbon dioxide and dioxygen ions were first identified by their full scan mass spectra on blanks at variable humidity levels (zero air with increasing amounts of deionized water (Millipore Corporation, Fontenay-sous-bois, France), in order to identify all the clusters formed with each precursor ion. The different ions formed with the negative precursors in presence of air and water are gathered in Supplementary Information, Table S1. In the same way, the presence of methanol as stabilizer in the formaldehyde solution was considered in the identification of the product ions of formaldehyde.

Excluding ions arising from the matrix (Table S1), it is thus possible to identify the product ions from the target compounds. In the following section, these product ions (Table S1) were monitored using the single ion monitoring (SIM) mode.

4 – Experimental determination of the rate coefficients

The determination of precursor ion-analyte experimental rate coefficients requires the introduction of controlled and well-quantified analyte concentrations in the SIFT-MS instrument. Quantification using positive mode with product ions and rate constants already implemented in the software database (Supplementary Information, Table S2) was used simultaneously to control the gaseous atmosphere generation and the analytes concentration. Moreover for formaldehyde, the SIFT-MS positive mode calibration with the precursor ion H_3O^+ was successfully compared to the standardized method (DNPH-HPLC) as shown in Figure S1. Negative primary product ions previously identified in full scan records were specifically monitored using the SIM mode. Successive positive and negative ionization spectra were recorded in the same scan with an integration time of 60 s in each case.

Rate coefficients were determined over a wide range of concentrations from a few ppb to a few ppm for each individual compound and correspond to the average of the values for each concentration (repeated three times) of the range (Table 3). The uncertainty in the experimental rate constants is less than 20%.

Rate coefficients were calculated for each concentration according to the following equation (Eq. 2):⁴⁸

$$k = \frac{P^- \times ICF_P}{[A] \times t_r \times R^- \times ICF_R} \quad (\text{Eq. 2})$$

k : rate coefficient ($\text{cm}^3 \text{ molecules}^{-1} \text{ s}^{-1}$)

t_r : reaction time in the flow tube, measured by the instrument (s)

P^- : primary product ion signal, measured by the instrument (Hz)

R^- : precursor ion signal, measured by the instrument (Hz)

ICF_P : Instrument Calibration Function of product ion, dependent on the instrument

ICF_R : Instrument Calibration Function of precursor ion, dependent on the instrument

$[A]$: analyte concentration in the flow tube (molecules cm^{-3}),

The analyte concentration depends on the sample concentration (*i.e.* analyte concentration in the Tedlar bag) according to Eq. 3:

$$[A] = C_{ppb} \times \frac{\Phi_s}{(\Phi_s + \Phi_c)} \times \frac{P_{FT}}{k_B \times T_{FT} \times 10^{15}} \quad (\text{Eq. 3})$$

C_{ppb} : sample concentration (ppb)

Φ_s : sample flow rate ($\text{m}^3 \text{ s}^{-1}$)

Φ_c : carrier gas flow rate ($\text{m}^3 \text{ s}^{-1}$)

P_{FT} : flow tube pressure (Pa)

T_{FT} : flow tube temperature (K)

k_B : Boltzmann constant ($\text{m}^2 \text{ kg s}^{-2} \text{ K}^{-1}$)

5 – Determination of the branching ratio

Ion-molecule reactions may have multiple product channels. The ratio of the product channels is the branching ratio. The primary product branching ratios of the reactions with the different negative precursor ions were determined by plotting the percentages of the individual product ion count rate (recorded in SIM mode) on a linear scale as a function of the total product ions count rate (varied by modifying the analyte concentration). Branching ratio corresponds to the percentage of the individual product ion count rate when the total product ions count rate is zero. By extrapolating the linear plot to zero signal, the true primary branching ratios, excluding any secondary reactions can be obtained. An example of determination of the branching ratio is presented in Supplementary Information, Figure S2.

6 - Secondary reactions: water and analyte clusters

In the flow tube, secondary reactions may occur between primary product ions and water to lead to the formation of water-analyte cluster ions. The influence of water on their formation was analysed for each target compounds (aldehydes and carboxylic acids) by recording SIM scans at variable humidity levels and constant analyte concentration (by spiking increasing amounts of water in the Tedlar bag), monitoring the intensity of secondary ions signal. Water clusters and analyte clusters were thus considered and the dependence of water cluster intensity as a function of humidity in the specific case of formaldehyde and butanal is shown in Supplementary Information (Figure S3). The general trend is the increase of the water-analyte cluster ion with increasing RH.

Computational details

Reaction paths of the reactions experimentally observed with OH⁻ as the reactant ion were calculated with the Hartree-Fock (HF), MP2 and CCSD(t) single point methods using the triple zeta basis set 6-311++g(d,p). All calculations were carried out using the Gaussian09 program⁴⁹. Geometry optimisations were carried out without any symmetry restrictions in the gas phase. The nature of the minima and transition states (TS) was verified with analytical frequency calculations, by the absence or presence of only one negative eigenvalue respectively. IRC calculations were used to confirm the connection between the TS and the corresponding minima. The parameters necessary for the calculation of the collisional rate constants (dipole moment μ_r and polarizability α of the neutral) were calculated at the MP2/6-311++g(d,p) level of theory.

Results and discussion

1 – Reactions in the flow tube

1.1 – OH⁻ reactions

Aldehydes

Full scan SIFT-MS analysis showed that aldehydes react with OH⁻ and this reaction leads to the formation of different product ions, summarized in Table 1. With all the studied aldehydes, including benzaldehyde, deprotonation occurs as the single reaction pathway with OH⁻ (*i.e.* a branching ratio of 100%), thus forming [M-H]⁻ ions according to Equation 4.



However, these ions are not the only ones observed in the SIFT-MS analysis of aldehydes. In the presence of water in the flow tube, [M-H]⁻ ions can be hydrated thus forming secondary ions at m/z M+17 with an intense signal according to Equation 5. This reaction is dependent on the amount of water in the flow tube, *i.e.* residual water in the system, water generated by Equation 4 and mostly water from the sample (Figure S3). Sample humidity therefore has an influence on the measurement and these hydrated ions must be included for the accurate quantification of aldehydes by SIFT-MS. Only for acetaldehyde, this hydrated ion (m/z 61) could not be observed experimentally because of interference with CO₂ from the air that reacts with OH⁻ to form ion at m/z 61 (Supplementary Information, Table S1). Thus, unlike other aldehydes, acetaldehyde hydrate was later neglected for the determination of reaction coefficients and quantification.



It should be noted that water can also react with OH⁻ reagent ion in the flow tube according to Equation 6. Thus, it can be considered that the [M-H]⁻ ion comes from reaction between the aldehyde and OH⁻.H₂O ion. However, this hydrate formation channel is neglected here since reaction 6 is very slow ($k=1.1 \times 10^{-12} \text{ cm}^3 \text{ s}^{-1}$) compared to reaction 5 (Table 3).

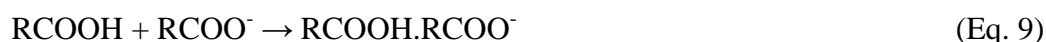
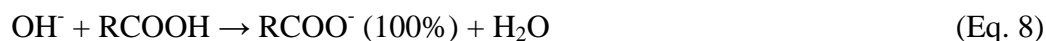


In the flow tube, [M-H]⁻ ions can also react with unreacted aldehyde molecules. This reaction leads to secondary ions at m/z M.[M-H]⁻ according to Equation 7, with a negligible intensity compared to primary ions and water clusters (<10% of the total signal). The M.[M-H]⁻ analyte cluster was not detected for hexanal. However, considering these analyte clusters could allow a better accuracy in the aldehyde's quantification.



Carboxylic acids

The very favourable reaction of carboxylic acids with OH⁻ results in two product ions. As with aldehydes, deprotonation occurs as the single channel in the primary reaction (Equation 8) and leads to a stable product ion RCOO⁻, with a branching ratio of 100%. In this case, hydration of primary product ion does not occur even by increasing water concentration in the flow tube, while the formation of carboxylic acid clusters is only observed for the lightest ones (formic and acetic acids), as for aldehydes (Equation 9).



1.2 – O^{•-} and O₂^{•-} reactions

Experimentally, deprotonation of aldehydes only occurs by reaction with O^{•-} and O₂^{•-} precursors leading to [M-H]⁻ primary ions (with a branching ratio of 100%). As with OH⁻, it is also possible to observe the formation of water clusters in the presence of water in the flow tube, but with a lower intensity. Indeed, in this case, no water is produced from the ion-aldehyde reaction (Eqs 10 and 11). In addition, since the precursor O^{•-} is generated from dry air, there is generally no or little residual water in the system and the hydration reaction is directly related to the sample humidity. The reaction between primary ions and unreacted aldehydes leading to analyte clusters at m/z M.[M-H]⁻, is also observed as with OH⁻.



The reaction of carboxylic acids with O^{•-} and O₂^{•-} results in two product ions, the major one at m/z [M-H]⁻ resulting from deprotonation (Eqs 10 and 11). The second product ion at m/z M.[M-H]⁻ results directly from secondary reactions with unreacted carboxylic acid molecules.

1.3 – NO₂⁻ and NO₃⁻ reactions

With NO₃⁻ precursor, product ion was detected neither from aldehydes nor from carboxylic acids, indicating that there is no reaction in the flow tube between NO₃⁻ and these compounds, or that these reactions have a small rate constant (lower than 10⁻¹¹ cm³ s⁻¹). The same holds true for the reaction between NO₂⁻ and aldehydes. However, reaction between carboxylic acids and NO₂⁻ results in two product ions from two different reaction channels: either proton abstraction leading to *m/z* [M-H]⁻ ion according to Equation 12, or an ion-molecule association thus forming M.NO₂⁻ ions (Equation 13) as the major pathway, still favoured with longer carboxylic acid chains (Table 2).



2 – SIFT-MS negative ionization for quantification of aldehydes and carboxylic acids

SIFT-MS quantification requires the knowledge of the reaction rate constant *k* (Eq. 1). From the numerous studies in the positive mode SIFT-MS, it is well known that proton transfer reactions from H₃O⁺ proceed at the gas kinetic (collisional) rate *k_c*, when these reactions are exothermic by more than 40 kJ mol⁻¹ ^{50,51}, an assumption which is well justified by numerous experiments ⁵². Accordingly, in the literature, the experimentally determined rate coefficients are often compared to the collisional rate constant (*k_c*) ^{53(p),54-56}, calculated according to parametrised trajectory calculations using the dipole moment μ_r and polarizability α of the neutral, and the reduced mass of the collisional ion-molecule partners ⁵⁷. The experimental *k* values were determined from known concentrations of aldehydes and carboxylic acids while collisional rate constants, *k_c*, could be estimated according to the method described by Su and Chesnavich derived from the polarizability α and the dipole moment μ_D of the neutral derived from MP2/6-311++g(d,p) calculations ⁵⁷. The corresponding data are summarized in Table 3. The rate constant must be high enough (greater than 10⁻¹⁰ in this study) for a sensitive detection of product ions and thus accurate quantification. These conditions are fulfilled in negative ionization for most aldehydes and carboxylic acids. In the case of formaldehyde, the quantification with any negative precursor is less accurate due to the much smaller value of the reaction rate constant (*k* = 4.3 × 10⁻¹¹ cm³ s⁻¹ with OH⁻, Figure S4). Thus, SIFT-MS negative ionization opens new possibilities for aldehydes (except formaldehyde) and carboxylic acids measurement in complex gaseous matrices. OH⁻ and O₂^{•-} are the most reactive negative precursors with both series of compounds with the highest rate constants, in the range 10⁻⁹ – 10⁻¹⁰ cm³ s⁻¹. When comparing the positive and negative modes, the reaction rate constant of acetaldehyde with H₃O⁺ (*k* = 7.4 × 10⁻¹⁰ cm³ s⁻¹, Table S2) and with OH⁻ (*k* = 1.4 × 10⁻⁹ cm³ s⁻¹, Table 3) are of the same order of magnitude. The same holds true for the reaction of formic acid (*k* = 2.3 × 10⁻⁹ cm³ s⁻¹ with O₂^{•-}, Table 3) against *k* = 2.2 × 10⁻⁹ cm³ s⁻¹ with H₃O⁺ (Table S2), with similar limits of detection (LOD), respectively 15.2 and 22.7 ppb, making the negative mode highly relevant for low-concentration of this acid in complex mixtures, as shown below. As expected, it can be noted that, owing to the presence of their labile hydrogen and to a very favorable primary deprotonation leading to stable carboxylate ions, the reaction is much faster between carboxylic acids and O^{•-} and mainly with O₂^{•-} than with aldehydes. SIFT-MS negative ionization is thus particularly suitable for volatile carboxylic acids analysis.

Starting from these experimentally determined rate constants in the negative mode, the analyte quantification was possible and the correspondence between the concentration

measured by negative ionization and the expected concentration derived from the simultaneous positive mode measurement on selected examples is presented in Supplementary Information, Figure S4. The correlation between the obtained concentrations and the expected ones is more accurate with increasing k values, with a noticeably bad result in the case of the poorly reactive formaldehyde.

Several of the reaction studied in this work have been previously examined by flowing afterglow and/or SIFT-MS.^{53,56,58,59} Product ions reported in the literature are sometimes different from those observed experimentally in this study. For instance, Bohme *et al.* indicates the formation of a HCO_2^- ion ($m/z = 45$) from the reaction of formaldehyde with O^- precursor,⁵⁸ which was not observed here. Differences are also noted in k values. Spanel *et al.* and Tanner *et al.* indicate rate constants k of 3.9×10^{-9} and $3.1 \times 10^{-9} \text{ cm}^3 \text{ s}^{-1}$, respectively, for the reaction between OH^- precursor and acetaldehyde.^{53,56} However, in all these cases the experimental conditions are significantly different from ours. First, from one study to another, the temperature of the flow tube varies between 140 and 300 K against 392 K in the present work. Second, the most significant difference arises from the carrier gas: previous studies used helium or hydrogen, whereas in the present work the carrier gas was nitrogen (N_2). Because of these significantly different experimental conditions, the comparison of absolute experimental rate constants from the literature with our results is not relevant. Nonetheless, the determination of the rate constants of negative ion-molecule reactions under our SIFT-MS conditions was necessary to better understand **the relative reactivity** of aldehydes and acids and to develop the most adapted analytical methods.

The calculated energies of the studied reactions, from the following starting aldehydes (formaldehyde, acetaldehyde, propanal and benzaldehyde) to the final anions are summarized in Table S3. In all cases, aldehyde deprotonation from $\text{M} + \text{OH}^-$ to $[\text{M-H}]^- + \text{H}_2\text{O}$ is either weakly exothermic (formaldehyde) or weakly endothermic (Table S3). Thus, the calculation of the surface energy potential (SEP) shows that the corresponding product anions RCO^- are not thermodynamically favoured, although experimentally observed due to the experimental conditions in the flow tube (400 K). Indeed, an aldehyde complex $[\text{RCOH.OH}]^-$ is always found on the potential energy surface (PES), which thermodynamically stabilized the system (-19 to -27 kcal mol^{-1} from acetaldehyde to benzaldehyde). Relative to the isolated partners RCOH and OH^- taken as starting reagents (0 kcal mol^{-1}), we observe an increase of the barrier between the stabilized complex $[\text{RCOH.OH}]^-$ and the transition state (TS) from acetaldehyde to benzaldehyde (5 to 8 kcal mol^{-1}) suggesting, in this first approach, an easier reaction for acetaldehyde than for benzaldehyde. It is noteworthy that the investigated formation of $[\text{RCO}^- \cdot \text{H}_2\text{O}]$ complexes from the $[\text{RCOH.OH}]^-$ ones corresponds to an endothermic reaction. However, for formaldehyde, the reversibility of the reaction could not be excluded considering the low energy involved in the back process (1.71 kcal mol^{-1} from the anion complex $[\text{RCO}^- \cdot \text{H}_2\text{O}]$ to the corresponding TS, compared to $\approx 3 \text{ kcal mol}^{-1}$ for the complexes with other aldehydes, see Figure 1). This result may tentatively explain the lower experimental k value for formaldehyde than for the other aldehydes.

Since it has been reported that aldehydes react with OH^- by proton extraction of hydrogen from the CH_x group alpha to the carbonyl group⁵³, we also need to consider this possible reactivity. In this case, the TS corresponding to this reaction could not be found in the PES using MP2 in contrast with HF level, corresponding to a very flat surface. In fact, the TS is found (using HF) at $\approx 1 \text{ kcal mol}^{-1}$ for the acetaldehyde alpha H reaction with OH^- . The same absence of TS also appears with the acid derivatives. In the acid case, two reactions must be considered: i) the reactions with the acidic proton; ii) the reactions with the hydrogen in alpha position. As expected, the first reactions lead to thermodynamically more favoured

products ($-60 \text{ kcal mol}^{-1}$) than the corresponding anion resulting from the abstraction of the proton on the carbon atom in alpha position ($-18 \text{ kcal mol}^{-1}$ for acetic acid).

Except for formaldehyde, the strong exothermicity of the alpha hydrogen abstraction from aldehydes and of acid deprotonation accounts for the experimental observations and high k values, which are of the same order of magnitude in both cases. The stabilization of the $[\text{RCO}^-\cdot\text{H}_2\text{O}]$ complex is consistent with the experimental observation of both the anion and its hydrate (Table 1).

It may be noted that calculated k_c appears insufficient to account for the experimental k , which involves both the collision between the reactants and the energy profile of the reaction. Indeed, for formaldehyde and benzaldehyde, which lack hydrogen on the α carbon, the experimental rate constants are the farthest from the calculated collisional rate constant k_c . The experimental k value is related to a given m/z value for $[\text{M-H}]^-$, but does not give any information on the structure of the ion, *i.e.* CH_3CO^- vs CH_2^-COH in the case of acetaldehyde, while for formaldehyde and benzaldehyde, only one structure is possible. It may be assumed that in these two cases, the exothermic alpha H abstraction is not possible, implying that the collision complex does not lead so easily to the formation of reaction products.

3 – Applications

3.1 – Determination of formic acid in formaldehyde

Aldehydes oxidation leads to the formation of carboxylic acids and accordingly, formic acid can be found as an impurity at low concentration in formaldehyde solutions. Since SIFT-MS negative ionization analysis of carboxylic acids was previously shown from the reaction rate constants to be highly efficient, the presence of formic acid has been investigated in a solution of formaldehyde by this method. To this end, different volumes of a commercial solution of formaldehyde (37% wt. in water) was spiked in a 1 L Tedlar bag filled with dry clean air. Full scan and SIM spectra were recorded and concentrations were measured using previously determined product ions (Table 1) and reaction rate coefficients (Table 3). Formaldehyde was quantified with H_3O^+ ion precursor (according to Table S2) whereas formic acid was quantified with the most reactive O_2^- ion precursor. Figure 2 shows a full scan mass spectrum of a commercial solution formaldehyde. The major signals correspond to O_2^- ion precursor (m/z 32) and its cluster ion with water (m/z 50, Table S1). As expected, product ions 29 and 47 corresponding to formaldehyde (Table 1) are detected. However, it is found that m/z 45 ion corresponding to formic acid is also detected. The signal of this latter is much more intense (6250 Hz) than those corresponding to formaldehyde (75 and 1875 Hz, for product ions 29 and 47, respectively), which is nevertheless the major compound after water in the solution. The high reactivity of formic acid with O_2^- ion precursor ($k = 2.3 \times 10^{-9} \text{ cm}^3 \text{ s}^{-1}$) compared to the lower rate constant of formaldehyde ($k = 1.4 \times 10^{-11} \text{ cm}^3 \text{ s}^{-1}$) accounts for the relative intensities of these signals.

The concentrations of formaldehyde generated from this same solution were then measured as well as any traces of formic acid (Table S4). These results clearly show the presence of formic acid in the formaldehyde solution. The concentration of this impurity represents about 4% of the formaldehyde concentration. This result warns about the conservation conditions of formaldehyde aqueous solutions, and more generally, of aldehyde solutions.

With standard methods of formaldehyde analysis such as DNPH cartridges, it is not possible to detect formic acid. SIFT-MS technology negative ionization offers a real

advantage here for the simultaneous detection of formic acid as an impurity of formaldehyde in a single experiment. Indeed, the difference in reactivity between formaldehyde and formic acid with the negative precursors, and in particular O_2^- precursor, makes it possible to detect quite easily the presence of formic acid in such a formaldehyde-rich matrix.

3.2 – Simultaneous analysis of aldehydes and carboxylic acids

Current applications for air quality need the analysis of aldehydes and carboxylic acids at the same time. A SIFT-MS analysis method has been developed for the investigation of VOCs emission from building materials using the previously obtained results (sections 1-3) and its details are summarized in Table 4. Emission rates from building materials were determined in emission chamber after 3 and 28 days according to the several standards NF ISO 16000. Air of emission chamber was sampled using Tedlar bag and then analysed by SIFT-MS. The emission rate of linoleum-type materials thus obtained are given in Supplementary Information, Table S5 and were confirmed by standard analytical methods

Due to some interferences between the product ions (a given precursor ion leads to the same primary or secondary product ion with different compounds), simultaneous analysis of all these compounds was not possible using only positive ionization. Here, the combined use of positive and negative ionization allowed the simultaneous analysis of a series of aldehydes (C1-C7) and carboxylic acids (C1-C6) in single scan experiments. For this method, precursor ions were selected according to their high enough rate constant ($k > 10^{-10} \text{ cm}^3 \text{ s}^{-1}$), moreover avoiding interferent product ions. The limits of detection (LOD) of the studied aldehydes and carboxylic acids were determined and are presented in Table 4 in comparison with other conventional methods for aldehydes and carboxylic acids analysis.

If the sensitivity is better for aldehydes analysis with standard methods (Table 4), the detection limits obtained with SIFT-MS remains in agreement with conventional applications. However, except for formic acid, sensitivity remains better for the analysis of carboxylic acids by SIFT-MS than ion chromatography methods. In addition, SIFT-MS analyses are simpler and faster to implement. While the measurement of aldehydes and carboxylic acids conventionally requires at least three different methods (DNPH cartridge sampling followed by HPLC analysis for some aldehydes, sorbent tube sampling followed by thermal desorption and GC-MS analysis for other aldehydes and ion chromatography for carboxylic acids, see Table 4), only one is sufficient by SIFT-MS.

This application demonstrates the relevance of SIFT-MS for the simultaneous analysis of aldehydes and carboxylic acids. The development of SIFT-MS negative ionization opens up thus new possibilities in terms of aldehydes and carboxylic acids analysis in air. However, it is important to note that, despite these new possibilities brought about by the combination of the two ionization modes (positive and negative), interferences are still possible. Isobaric compounds can be adequately monitored by the different precursor ions of SIFT-MS as long as they bear different functional groups (for instance $HCOOCH_3$ vs CH_3COOH or CH_3CH_2COH vs CH_3COCH_3). Completing the database with the largest range of precursor ions is the best solution to identify the interferences and to increase the resolution of the method. However, the analysis of mixtures containing regio-isomeric compounds is indeed a limitation of SIFT-MS as shown by Smith et al. for the analysis of isomers of hexanol. Regio-isomers **may possibly** react differently depending on the precursor ion but this is not the general case.⁶⁰

Conclusion

The aim of the present work was to determine the potential contribution of negative ionization for aldehydes and carboxylic acids quantification in air by SIFT-MS. Reactivity with the different negative precursor ions was studied experimentally. Theoretical modeling was used for a better understanding of ion-molecule reaction paths. The experimental reaction rate constants k were found very different from the calculated collisional rate constants k_c , which did not appear to be relevant for estimating experimental reaction rate constants. In any case, SIFT-MS negative ionization is particularly suitable for the analysis of carboxylic acids and aldehydes, with the exception of formaldehyde, with high rate constants and sensitivity comparable to that obtained in positive ionization. However, the greatest strength of negative ionization is to extend the range of analysis possibilities of complex mixtures by SIFT-MS. The combined use of positive and negative ionization allows the quantification of aldehydes and carboxylic acids simultaneously and without interference between these compounds. SIFT-MS technology simplifies the analysis of these compounds which can be much more time-consuming with traditional methods. Thus, the analysis of aldehydes and carboxylic acids in the gas phase can be done fast and simply, without sample preparation, in a single experiment.

Acknowledgements

Authors thank Conseil Régional Nouvelle Aquitaine (CRNA) and Interscience for financial support of this work in the frame of POLLIMPACT project.

References

1. Kim J, Kim S, Lee K, Yoon D, Lee J, Ju D. Indoor aldehydes concentration and emission rate of formaldehyde in libraries and private reading rooms. *Atmospheric Environment*. 2013;71:1-6. doi:10.1016/j.atmosenv.2013.01.059
2. OQAI. *Final Report, Hiérarchisation Sanitaire Des Paramètres d'intérêt Pour l'Observatoire de La Qualité de l'Air Intérieur : Application Aux Phtalates, Paraffines Chlorées à Chaîne Courte, Organo-Étains, Alkyl Phénols et Retardateurs de Flamme Bromés.*; 2005. http://www.oqai.fr/userdata/documents/Document_13.pdf. Accessed January 8, 2019.
3. Tsai W-T. An overview of health hazards of volatile organic compounds regulated as indoor air pollutants. *Reviews on Environmental Health*. 2019;34(1):81-89. doi:10.1515/reveh-2018-0046
4. Karakitsios S, Asikainen A, Garden C, et al. Integrated exposure for risk assessment in indoor environments based on a review of concentration data on airborne chemical pollutants in domestic environments in Europe. *Indoor and Built Environment*. 2015;24(8):1110-1146. doi:10.1177/1420326X14534865
5. Plaisance H, Blondel A, Desauziers V, Mocho P. Characteristics of formaldehyde emissions from indoor materials assessed by a method using passive flux sampler measurements. *Building and Environment*. 2014;73:249-255. doi:10.1016/j.buildenv.2013.12.011
6. Jiang C, Li D, Zhang P, Li J, Wang J, Yu J. Formaldehyde and volatile organic compound (VOC) emissions from particleboard: Identification of odorous compounds and effects of heat treatment. *Building and Environment*. 2017;117:118-126. doi:10.1016/j.buildenv.2017.03.004
7. Que Z-L, Wang F-B, Li J-Z, Furuno T. Assessment on emission of volatile organic compounds and formaldehyde from building materials. *Composites Part B: Engineering*. 2013;49:36-42. doi:10.1016/j.compositesb.2013.01.008
8. Weschler CJ. Changes in indoor pollutants since the 1950s. *Atmospheric Environment*. 2009;43(1):153-169. doi:10.1016/j.atmosenv.2008.09.044
9. Weschler CJ. Ozone in Indoor Environments: Concentration and Chemistry. *Indoor Air*. 2000;10(4):269-288. doi:10.1034/j.1600-0668.2000.010004269.x
10. Fadeyi MO. Ozone in indoor environments: Research progress in the past 15 years. *Sustainable Cities and Society*. 2015;18:78-94. doi:10.1016/j.scs.2015.05.011
11. Liu D, Nyord T, Rong L, Feilberg A. Real-time quantification of emissions of volatile organic compounds from land spreading of pig slurry measured by PTR-MS and wind tunnels. *Science of The Total Environment*. 2018;639:1079-1087. doi:10.1016/j.scitotenv.2018.05.149
12. Parker DB, Gilley J, Woodbury B, et al. Odorous VOC emission following land application of swine manure slurry. *Atmospheric Environment*. 2013;66:91-100. doi:10.1016/j.atmosenv.2012.01.001

13. Walgraeve C, Van Huffel K, Bruneel J, Van Langenhove H. Evaluation of the performance of field olfactometers by selected ion flow tube mass spectrometry. *Biosystems Engineering*. 2015;137:84-94. doi:10.1016/j.biosystemseng.2015.07.007
14. Castada HZ, Wick C, Taylor K, Harper WJ. Analysis of Selected Volatile Organic Compounds in Split and Nonsplit Swiss Cheese Samples Using Selected-Ion Flow Tube Mass Spectrometry (SIFT-MS). *Journal of Food Science*. 2014;79(4):C489-C498. doi:10.1111/1750-3841.12418
15. Taylor K, Wick C, Castada H, Kent K, Harper WJ. Discrimination of Swiss Cheese from 5 Different Factories by High Impact Volatile Organic Compound Profiles Determined by Odor Activity Value Using Selected Ion Flow Tube Mass Spectrometry and Odor Threshold. *Journal of Food Science*. 2013;78(10):C1509-C1515. doi:10.1111/1750-3841.12249
16. Langford VS, Reed CJ, Milligan DB, McEwan MJ, Barringer SA, Harper WJ. Headspace Analysis of Italian and New Zealand Parmesan Cheeses. *Journal of Food Science*. 2012;77(6):C719-C726. doi:10.1111/j.1750-3841.2012.02730.x
17. Langford V, Gray J, Foulkes B, Bray P, McEwan MJ. Application of Selected Ion Flow Tube-Mass Spectrometry to the Characterization of Monofloral New Zealand Honeys. *Journal of Agricultural and Food Chemistry*. 2012;60(27):6806-6815. doi:10.1021/jf3025002
18. Brändle J, Domig KJ, Kneifel W. Relevance and analysis of butyric acid producing clostridia in milk and cheese. *Food Control*. 2016;67:96-113. doi:10.1016/j.foodcont.2016.02.038
19. Lourenço C, González-Méndez R, Reich F, Mason N, Turner C. A potential method for comparing instrumental analysis of volatile organic compounds using standards calibrated for the gas phase. *International Journal of Mass Spectrometry*. 2017;419:1-10. doi:10.1016/j.ijms.2017.05.011
20. Lourenço C, Turner C. Breath Analysis in Disease Diagnosis: Methodological Considerations and Applications. *Metabolites*. 2014;4(2):465-498. doi:10.3390/metabo4020465
21. Vogel M, Büldt A, Karst U. Hydrazine reagents as derivatizing agents in environmental analysis - a critical review. *Fresenius' Journal of Analytical Chemistry*. 2000;366(8):781-791. doi:10.1007/s002160051572
22. Salthammer T, Mentese S. Comparison of analytical techniques for the determination of aldehydes in test chambers. *Chemosphere*. 2008;73(8):1351-1356. doi:10.1016/j.chemosphere.2008.06.054
23. Szulejko JE, Kim K-H. Derivatization techniques for determination of carbonyls in air. *TrAC Trends in Analytical Chemistry*. 2015;64:29-41. doi:10.1016/j.trac.2014.08.010
24. Diodiu R, Dogeanu A. Development and Validation of an Analytical Method for Quantitative Determination of Carboxylic Acids in Air Samplers. *Energy Procedia*. 2016;85:201-205. doi:10.1016/j.egypro.2015.12.217
25. Majchrzak T, Wojnowski W, Lubinska-Szczygeł M, Róžańska A, Namieśnik J,

- Dymerski T. PTR-MS and GC-MS as complementary techniques for analysis of volatiles: A tutorial review. *Analytica Chimica Acta*. 2018;1035:1-13. doi:10.1016/j.aca.2018.06.056
26. Cappellin L, Aprea E, Granitto P, et al. Linking GC-MS and PTR-TOF-MS fingerprints of food samples. *Chemometrics and Intelligent Laboratory Systems*. 2012;118:301-307. doi:10.1016/j.chemolab.2012.05.008
27. Bourdin D, Desauziers V. Development of SPME on-fiber derivatization for the sampling of formaldehyde and other carbonyl compounds in indoor air. *Anal Bioanal Chem*. 2014;406(1):317-328. doi:10.1007/s00216-013-7460-6
28. Song H, Liu J. GC-O-MS technique and its applications in food flavor analysis. *Food Research International*. 2018;114:187-198. doi:10.1016/j.foodres.2018.07.037
29. Biasioli F, Yeretizian C, Märk TD, Dewulf J, Van Langenhove H. Direct-injection mass spectrometry adds the time dimension to (B)VOC analysis. *TrAC Trends in Analytical Chemistry*. 2011;30(7):1003-1017. doi:10.1016/j.trac.2011.04.005
30. Smith D, Španěl P, Herbig J, Beauchamp J. Mass spectrometry for real-time quantitative breath analysis. *Journal of Breath Research*. 2014;8(2):027101. doi:10.1088/1752-7155/8/2/027101
31. Sovová K, Dryahina K, Španěl P. Selected ion flow tube (SIFT) studies of the reactions of H₃O⁺, NO⁺ and O₂⁺ with six volatile phytogetic esters. *International Journal of Mass Spectrometry*. 2011;300(1):31-38. doi:10.1016/j.ijms.2010.11.021
32. Gibson A, Malek L, Dekker RFH, Ross B. Detecting volatile compounds from Kraft lignin degradation in the headspace of microbial cultures by selected ion flow tube mass spectrometry (SIFT-MS). *Journal of Microbiological Methods*. 2015;112:40-45. doi:10.1016/j.mimet.2015.03.008
33. Shestivska V, Olšinová M, Sovová K, et al. Evaluation of lipid peroxidation by the analysis of volatile aldehydes in the headspace of synthetic membranes using selected ion flow tube mass spectrometry. *Rapid Communications in Mass Spectrometry*. 2018;32(18):1617-1628. doi:10.1002/rcm.8212
34. Španěl P, Dryahina K, Smith D. A general method for the calculation of absolute trace gas concentrations in air and breath from selected ion flow tube mass spectrometry data. *International Journal of Mass Spectrometry*. 2006;249:230-239. doi:10.1016/j.ijms.2005.12.024
35. Wang T, Španěl P, Smith D. Selected ion flow tube mass spectrometry of 3-hydroxybutyric acid, acetone and other ketones in the headspace of aqueous solution and urine. *International Journal of Mass Spectrometry*. 2008;272(1):78-85. doi:10.1016/j.ijms.2008.01.002
36. Biasioli F, Gasperi F, Yeretizian C, Märk TD. PTR-MS monitoring of VOCs and BVOCs in food science and technology. *TrAC Trends in Analytical Chemistry*. 2011;30(7):968-977. doi:10.1016/j.trac.2011.03.009
37. Ting VJL, Romano A, Soukoulis C, et al. Investigating the in-vitro and in-vivo flavour release from 21 fresh-cut apples. *Food Chemistry*. 2016;212:543-551.

doi:10.1016/j.foodchem.2016.05.116

38. Zardin E, Tyapkova O, Buettner A, Beauchamp J. Performance assessment of proton-transfer-reaction time-of-flight mass spectrometry (PTR-TOF-MS) for analysis of isobaric compounds in food-flavour applications. *LWT - Food Science and Technology*. 2014;56(1):153-160. doi:10.1016/j.lwt.2013.10.041
39. Nenadis N, Heenan S, Tsimidou MZ, Van Ruth S. Applicability of PTR-MS in the quality control of saffron. *Food Chemistry*. 2016;196:961-967. doi:10.1016/j.foodchem.2015.10.032
40. Knížek A, Dryahina K, Španěl P, et al. Comparative SIFT-MS, GC-MS and FTIR analysis of methane fuel produced in biogas stations and in artificial photosynthesis over acidic anatase TiO₂ and montmorillonite. *Journal of Molecular Spectroscopy*. 2018;348:152-160. doi:10.1016/j.jms.2017.10.002
41. Michel E, Schoon N, Amelynck C, Guimbaud C, Catoire V, Arijs E. A selected ion flow tube study of the reactions of H₃O⁺, NO⁺ and O₂⁺ with methyl vinyl ketone and some atmospherically important aldehydes. *International Journal of Mass Spectrometry*. 2005;244(1):50-59. doi:10.1016/j.ijms.2005.04.005
42. Španěl P, Smith D. Progress in SIFT-MS: Breath analysis and other applications. *Mass Spectrom Rev*. 2011;30(2):236-267. doi:10.1002/mas.20303
43. Španěl P, Smith D. Account on the features, successes and challenges of selected ion flow tube mass spectrometry. *European Journal of Mass Spectrometry*. 2013;19(4):225. doi:10.1255/ejms.1240
44. Jordan A, Haidacher S, Hanel G, et al. An online ultra-high sensitivity Proton-transfer-reaction mass-spectrometer combined with switchable reagent ion capability (PTR+SRI-MS). *International Journal of Mass Spectrometry*. 2009;286(1):32-38. doi:10.1016/j.ijms.2009.06.006
45. Hera D, Langford V, McEwan M, McKellar T, Milligan D. Negative Reagent Ions for Real Time Detection Using SIFT-MS. *Environmets*. 2017;4(1):16. doi:10.3390/environments4010016
46. Harb P, Sivachandiran L, Gaudion V, Thevenet F, Locoge N. The 40 m³ Innovative experimental Room for INdoor Air studies (IRINA): Development and validations. *Chemical Engineering Journal*. 2016;306:568-578. doi:10.1016/j.cej.2016.07.102
47. O'Sullivan DW, Silwal IKC, McNeill AS, Treadaway V, Heikes BG. Quantification of gas phase hydrogen peroxide and methyl peroxide in ambient air: Using atmospheric pressure chemical ionization mass spectrometry with O₂⁻, and O₂⁻(CO₂) reagent ions. *International Journal of Mass Spectrometry*. 2018;424:16-26. doi:10.1016/j.ijms.2017.11.015
48. Španěl P, Smith D. Selected ion flow tube – mass spectrometry: detection and real-time monitoring of flavours released by food products. *Rapid Commun Mass Spectrom*. 1999;13(7):585-596. doi:10.1002/(SICI)1097-0231(19990415)13:7<585::AID-RCM527>3.0.CO;2-K
49. M.J. Frisch, G.W. Trucks, H.B. Schlegel, G.E. Scuseria, M.A. Robb, J.R. Cheeseman,

G. Scalmani, V. Barone, B. Mennucci, G.A. Petersson, H. Nakatsuji, M. Caricato, X. Li, H.P. Hratchian, A.F. Izmaylov, J. Bloino, G. Zheng, J.L. Sonnenberg, M. Hada, M. Ehara, K. Toyota, R. Fukuda, J. Hasegawa, M. Ishida, T. Nakajima, Y. Honda, O. Kitao, H. Nakai, T. Vreven, J. Montgomery J.A., J.E. Peralta, F. Ogliaro, M. Bearpark, J.J. Heyd, E. Brothers, K.N. Kudin, V.N. Staroverov, R. Kobayashi, J. Normand, K. Raghavachari, A. Rendell, J.C. Burant, S.S. Iyengar, J. Tomasi, M. Cossi, N. Rega, J.M. Millam, M. Klene, J.E. Knox, J.B. Cross, V. Bakken, C. Adamo, J. Jaramillo, R. Gomperts, R.E. Stratmann, O. Yazyev, A.J. Austin, R. Cammi, C. Pomelli, J.W. Ochterski, R.L. Martin, K. Morokuma, V.G. Zakrzewski, G.A. Voth, P. Salvador, J.J. Dannenberg, S. Dapprich, A.D. Daniels, Ö. Farkas, J.B. Foresman, J.V. Ortiz, J. Cioslowski, D.J. Fox, Gaussian 09, Revision D.01, (2009).

50. Brůhová Michalčíková R, Španěl P. A selected ion flow tube study of the ion molecule association reactions of protonated (MH⁺), nitrosonated (MNO⁺) and dehydroxided (M–OH)⁺ carboxylic acids (M) with H₂O. *International Journal of Mass Spectrometry*. 2014;368:15-22. doi:10.1016/j.ijms.2014.04.010

51. Brůhová Michalčíková R, Dryahina K, Španěl P. A detailed study of the ion chemistry of alkenes focusing on heptenes aimed at their SIFT-MS quantification. *International Journal of Mass Spectrometry*. 2018;425:16-21. doi:10.1016/j.ijms.2017.12.004

52. Bouchoux G, Salpin JY, Leblanc D. A relationship between the kinetics and thermochemistry of proton transfer reactions in the gas phase. *International Journal of Mass Spectrometry and Ion Processes*. 1996;153(1):37-48. doi:10.1016/0168-1176(95)04353-5

53. Španěl P, Pavlik M, Smith D. Reactions of H₃O⁺ and OH[–] ions with some organic molecules; applications to trace gas analysis in air. *International Journal of Mass Spectrometry and Ion Processes*. 1995;145(3):177-186. doi:10.1016/0168-1176(95)04164-G

54. Španěl P, Smith D. Reactions of Hydrated Hydronium Ions and Hydrated Hydroxide Ions with Some Hydrocarbons and Oxygen-Bearing Organic Molecules. *J Phys Chem*. 1995;99(42):15551-15556. doi:10.1021/j100042a033

55. Španěl P, Ji Y, Smith D. SIFT studies of the reactions of H₃O⁺, NO⁺ and O₂⁺ with a series of aldehydes and ketones. *International Journal of Mass Spectrometry and Ion Processes*. 1997;165-166:25-37. doi:10.1016/S0168-1176(97)00166-3

56. Tanner SD, Mackay GI, Bohme DK. An experimental study of the reactivity of the hydroxide anion in the gas phase at room temperature, and its perturbation by hydration. *Canadian Journal of Chemistry*. 1981;59(11):1615-1621. doi:10.1139/v81-239

57. Su T, Chesnavich WJ. Parametrization of the ion–polar molecule collision rate constant by trajectory calculations. *The Journal of Chemical Physics*. 1982;76(10):5183-5185. doi:10.1063/1.442828

58. Bohme DK, Mackay GI, Tanner SD. An experimental study of nucleophilic addition to formaldehyde in the gas phase. *Journal of the American Chemical Society*. 1980;102(1):407-409. doi:10.1021/ja00521a084

59. Miller TM, Viggiano AA, Miller AES, et al. The formation and destruction of H₃O[–]. *The Journal of Chemical Physics*. 1994;100(8):5706-5714. doi:10.1063/1.467136

60. Smith D, Sovová K, Španěl P. A selected ion flow tube study of the reactions of H₃O⁺, NO⁺ and O₂^{+•} with seven isomers of hexanol in support of SIFT-MS. *International Journal of Mass Spectrometry*. 2012;319-320:25-30. doi:10.1016/j.ijms.2012.03.009

Table 1. The product ions for the reactions of OH^\bullet , O^\bullet and $\text{O}_2^{\bullet-}$ with aldehydes and carboxylic acids. In brackets, secondary products. Branching ratio 100 % in every case.

Compounds	MW	Formula	Products	<i>m/z</i>
Aldehydes				
Formaldehyde	30	CH_2O	CHO^-	29
			$(\text{CHO}^- \cdot \text{H}_2\text{O})$	(47)
			$(\text{CH}_2\text{O} \cdot \text{CHO}^-)$	(59)
Acetaldehyde	44	CH_3CHO	CH_3CO^-	43
			$(\text{CH}_3\text{CO}^- \cdot \text{H}_2\text{O})^a$	(61) ^a
			$(\text{CH}_3\text{CHO} \cdot \text{CH}_3\text{CO}^-)$	(87)
Butanal	72	$\text{C}_3\text{H}_7\text{CHO}$	$\text{C}_3\text{H}_7\text{CO}^-$	71
			$(\text{C}_3\text{H}_7\text{CO}^- \cdot \text{H}_2\text{O})$	(89)
			$(\text{C}_3\text{H}_7\text{CHO} \cdot \text{C}_3\text{H}_7\text{CO}^-)$	(143)
Hexanal	100	$\text{C}_5\text{H}_{11}\text{CHO}$	$\text{C}_5\text{H}_{11}\text{CO}^-$	99
Benzaldehyde	106	$\text{C}_6\text{H}_5\text{CHO}$	$\text{C}_6\text{H}_5\text{CO}^-$	105
			$(\text{C}_6\text{H}_5\text{CO}^- \cdot \text{H}_2\text{O})$	(123)
			$(\text{C}_6\text{H}_5\text{CHO} \cdot \text{C}_6\text{H}_5\text{CO}^-)$	(211)
Carboxylic acids				
Formic acid	46	HCOOH	HCOO^-	45
			$(\text{HCOOH} \cdot \text{HCOO}^-)$	(91)
Acetic acid	60	CH_3COOH	CH_3COO^-	59
			$(\text{CH}_3\text{COOH} \cdot \text{HCOO}^-)$	(119)
Butyric acid	88	$\text{C}_3\text{H}_7\text{COOH}$	$\text{C}_3\text{H}_7\text{COO}^-$	87
Caproic acid	116	$\text{C}_5\text{H}_{11}\text{COOH}$	$\text{C}_5\text{H}_{11}\text{COO}^-$	115

^a Could not be observed experimentally with OH^- precursor

Table 2. The product ions and the corresponding branching ratio (BR) for the reactions of NO_2^- with aldehydes and carboxylic acids.

Compounds	MW	Formula	NO_2^-		
			Products	<i>m/z</i>	BR (%)
Formic acid	46	HCOOH	HCOO ⁻	45	35
			HCOOH.NO ₂ ⁻	92	65
Acetic acid	60	CH ₃ COOH	CH ₃ COO ⁻	59	25
			CH ₃ COOH.NO ₂ ⁻	106	75
Butyric acid	88	C ₃ H ₇ COOH	C ₃ H ₇ COO ⁻	87	15
			C ₃ H ₇ COOH.NO ₂ ⁻	134	85
Caproic acid	116	C ₅ H ₁₁ COOH	C ₅ H ₁₁ COO ⁻	115	4
			C ₅ H ₁₁ COOH.NO ₂ ⁻	162	96

Table 3. Calculated collisional rate constants (k_c) and experimental (k) rate constants for the primary reactions of OH , O^\bullet , O_2^- and NO_2^- with aldehydes and carboxylic acids.

Compounds	MW ^a	Formula	α^a (10^{-24} cm^3)	μ_D^a (D)	OH^- k [k_c] ^b	O^- k [k_c] ^b	O_2^- k [k_c] ^b	NO_2^- k [k_c] ^b
Aldehydes								
Formaldehyde	30	CH_2O	2.26	2.98	0.04 [4.2]	0.004 [4.3]	0.01 [3.5]	- [3.2]
Acetaldehyde	44	$\text{C}_2\text{H}_4\text{O}$	4.11	3.37	1.4 [4.6]	0.2 [4.7]	0.09 [3.7]	- [3.4]
Propanal	58	$\text{C}_3\text{H}_6\text{O}$	5.82	3.48	2.2 [4.7]	0.2 [4.8]	0.07 [3.7]	- [3.4]
Butanal	72	$\text{C}_4\text{H}_8\text{O}$	7.60	3.54	2.3 [4.8]	0.2 [4.9]	0.3 [3.8]	- [3.4]
Hexanal	100	$\text{C}_6\text{H}_{12}\text{O}$	11.16	3.62	1.0 [5.0]	0.07 [5.1]	0.1 [3.8]	- [3.4]
Benzaldehyde	106	$\text{C}_7\text{H}_6\text{O}$	12.20	3.83	0.8 [5.2]	0.03 [5.9]	0.03 [4.0]	- [3.5]
Carboxylic acids								
Formic acid	46	CH_2O_2	2.98	1.67	0.8 [2.6]	0.5 [2.6]	2.3 [2.1]	0.2 [1.9]
Acetic acid	60	$\text{C}_2\text{H}_4\text{O}_2$	4.65	1.97	1.2 [3.0]	0.2 [3.0]	1.3 [2.4]	0.2 [2.1]
Butyric acid	88	$\text{C}_4\text{H}_8\text{O}_2$	8.14	2.17	1.0 [3.3]	0.3 [3.4]	1.7 [2.6]	0.5 [2.3]
Caproic acid	116	$\text{C}_6\text{H}_{12}\text{O}_2$	11.63	2.16	1.3 [3.5]	0.2 [3.5]	1.2 [2.7]	1.0 [2.3]

^a MW : molecular weight, α : polarizability, μ_r : dipole moment; both values calculated at MP2/6-311++g(d,p) level

^b Units: $10^{-9} \text{cm}^3 \text{s}^{-1}$

Table 4. SIFT-MS method vs classical methods for aldehydes and carboxylic acids analysis. Sampling of emission products from linoleum materials in Tedlar bags (SIFT-MS measurements).

	Standardized method			SIFT-MS method	
	sampling	analysis	LOD (ppb)	ionization mode	LOD (ppb)
Formaldehyde	DNPH cartridge	HPLC	0.61	+	11.3
Acetaldehyde	DNPH cartridge	HPLC	0.58	+ / -	4.58
Propanal	/	/	/	+	6.11
Butanal	Tenax	ATD-GC-MS	0.19	-	1.81
Pentanal	Tenax	ATD-GC-MS	0.09	+	4.50
Hexanal	Tenax	ATD-GC-MS	0.09	+ / -	3.92
Benzaldehyde	Tenax	ATD-GC-MS	0.05	+ / -	1.91
Formic acid	H ₂ O bubbler	Ion chromatography	4.78	+ / -	15.2
Acetic acid	H ₂ O bubbler	Ion chromatography	3.66	+ / -	3.38
Propanoic acid	H ₂ O bubbler	Ion chromatography	4.95	+	0.95
Butyric acid	H ₂ O bubbler	Ion chromatography	12.5	+ / -	1.18
Pentanoic acid	H ₂ O bubbler	Ion chromatography	14.4	+	14.4
Caproic acid	/	/	/	+ / -	0.76